Eur. J. Mineral.
2005, **17**, 129–141

Västmanlandite-(Ce) – a new lanthanide- and F-bearing sorosilicate mineral from Västmanland, Sweden: description, crystal structure, and relation to gatelite-(Ce)

DAN HOLTSTAM[1], UWE KOLITSCH[2] and ULF B. ANDERSSON[3]

[1]Sektionen för mineralogi, Naturhistoriska riksmuseet, Box 50007, SE-104 05 Stockholm, Sweden
Corresponding author, e-mail: dan.holtstam@nrm.se
[2]Institut für Mineralogie und Kristallographie, Universität Wien, Geozentrum, Althanstraße 14, A-1090 Wien, Austria
[3]Institutionen för geovetenskaper, Uppsala Universitet, Villavägen 16, SE-752 36 Uppsala, Sweden

Abstract: Västmanlandite-(Ce), ideally $(Ce,La)_3CaAl_2Mg_2[Si_2O_7][SiO_4]_3F(OH)_2$, is a new mineral species from the Västmanland county, Bergslagen region, Sweden. Together with more Fe-rich, F-poor members, it forms solid solutions that are important for lanthanide sequestration in the Bastnäs-type skarn deposits in Västmanland. At the type locality (Malmkärra, Norberg district) it occurs as anhedral grains 0.2–3 mm across, in association with fluorbritholite-(Ce), tremolite, a serpentine mineral, magnetite, dollaseite-(Ce) and dolomite. The mineral is allanite-like in appearance; it is dark brown, translucent, with vitreous luster, and has good cleavage parallel to {001}, uneven to conchoidal fracture, and a yellowish gray streak; D_{calc} = 4.51(2) g·cm^{-3} and Mohs hardness ≈ 6. Optically it is biaxial (-), with α = 1.781(4), β_{calc} = 1.792, γ = 1.810(4) and $2V_\alpha$ = 75(5)°. Chemical analysis by electron-microprobe and ^{57}Fe Mössbauer spectroscopy yield: La_2O_3 13.65, Ce_2O_3 23.90, Pr_2O_3 2.07, Nd_2O_3 6.28, Sm_2O_3 0.42, Gd_2O_3 0.15, Y_2O_3 0.18, CaO 4.65, FeO 1.14, Fe_2O_3 2.69, MgO 5.51, Al_2O_3 8.58, TiO_2 0.04, P_2O_5 0.05, SiO_2 26.61, F 1.06, H_2O_{calc} 1.61, O ≡ F –0.45, sum 98.14. Västmanlandite-(Ce) is monoclinic, $P2_1/m$, with a = 8.939(1), b = 5.706(1), c = 15.855(2) Å, β = 94.58(1)°, V = 806.1(2) Å^3, and Z = 2 (single-crystal data). The eight strongest lines in the X-ray powder diffraction pattern are [d (in Å) (I/I_0)(hkl)]: 15.81(16)(00$\bar{1}$), 4.65(10)(11$\bar{1}$), 3.50(20)(210), 2.983(100)(114), 2.685(13)(12$\bar{1}$), 2.678(11)(20$\bar{5}$), 2.625(19)(31$\bar{1}$), and 2.187(15)(40$\bar{2}$). The crystal structure was determined using single-crystal X-ray diffraction data and refined to $R1(F)$ = 1.73 % for 2864 'observed' reflections with $F_o > 4\sigma(F_o)$. Västmanlandite-(Ce) is nearly isotypic to gatelite-(Ce), ideally $Ce_3CaAl_2AlMg[Si_2O_7][SiO_4]_3O(OH)_2$, and can be described as a regular dollaseite-(Ce)–törnebohmite-(Ce) polysome. The occurrence of extremely weak, continuous streaking in the diffraction patterns, and the presence of two pairs of mirror-related atoms in the törnebohmite-(Ce) module indicate that the structure model represents an average structure, unlike the situation in gatelite-(Ce) where there are no continuous streaks but instead, due to atomic ordering, sharp superstructure reflections resulting in a different unit cell.

Key-words: västmanlandite-(Ce), new mineral species, crystal structure, polysome, gatelite-(Ce).

Introduction

In the Bergslagen mining region, south-central Sweden, a unique group of lanthanide mineralizations, referred to as Bastnäs-type deposits (Geijer, 1961; Holtstam & Broman, 2002), occurs clustered along a narrow NE-SW trending, *ca.* 80 km long zone. They consist of complex mineral assemblages of Fe-oxide ores, Ca-Mg-silicate skarns, lanthanide silicates, lanthanide fluorocarbonates and sulphides of Cu, Mo and Bi. The first deposits of this kind to be recognized are located in the Bastnäs ore field, which is regarded as the "birthplace" of no less than two chemical elements (Ce, La) and seven mineral species: cerite-(Ce), bastnäsite-(Ce), lanthanite-(Ce), linnaeite, törnebohmite-(Ce), cobaltkieserite and percleveite-(Ce) (Geijer, 1921; Holtstam, 2002; Holtstam *et al.*, 2003a).

A preliminary step in an ongoing research project, with the aim of obtaining a genetic model for this type of mineralization, was mineralogical characterization of selected samples. As a result, some potentially new mineral species were discovered, one of which was named västmanlandite-(Ce) after Västmanland, the county where the majority of the deposits are situated. This mineral, or in some cases an Fe analogue with which it forms solid solutions, has been found at several localities, and its presence can now be considered a characteristic feature of the Bastnäs-type deposits. Västmanlandite-(Ce) is nearly isotypic to the chemically related mineral gatelite-(Ce) (ideally $Ce_3CaAl_2AlMg[Si_2O_7][SiO_4]_3O(OH)_2$; Bonazzi *et al.*, 2003), which is comprised of epidote and törnebohmite-like structural modules.

The new mineral and its name have been approved by the IMA Commission on New Minerals and Mineral Names

DOI: 10.1127/0935-1221/2005/0017-0129
0935-1221/05/0017-0129 $ 5.85

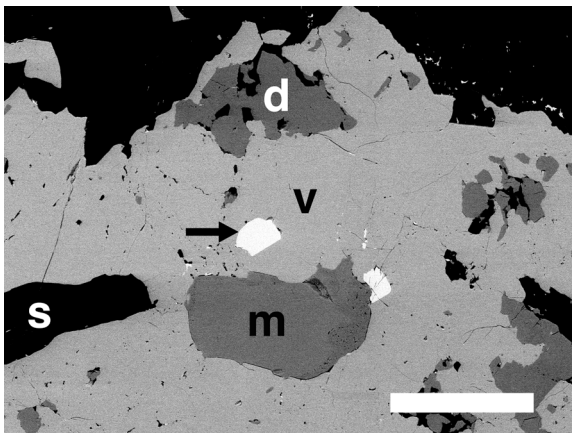

Fig. 1. Backscattered electron image of a portion of a västmanlandite-(Ce) (**v**) grain, with inclusions of magnetite (**m**), dollaseite-(Ce) (**d**) and serpentine plus relics of tremolitic amphibole (**s**). The arrow points to an inclusion of fluorbritholite-(Ce). The white scale bar equals 0.1 mm.

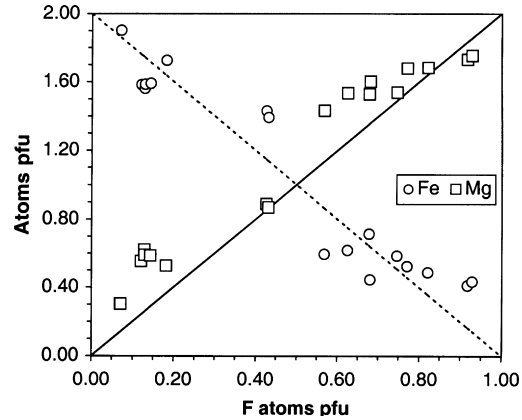

Fig. 2. Mg and Fe contents *vs.* F (atoms per formula unit) for all specimens for which average analytical data are given in Table 1. The solid and broken lines have a slope of 2 and –2, respectively.

(2002-025). Holotype material (cat. no. 01+0081) from the Malmkärra mine, Norberg district, Västmanland (lat. 60°3'N, long. 15°51'E) and other specimens referred to, including a number of polished thin sections, are in the mineral collection of the Swedish Museum of Natural History, Stockholm.

Geological setting and occurrences

The Precambrian geology of Västmanland and adjacent areas (which belong to the central part of Bergslagen), can be summarized as follows (Ambros, 1983, 1988; Allen *et al.*, 1996; Persson, 1997; Ripa *et al.*, 2002): The oldest identified bedrock comprises metavolcanic and metasedimentary rocks of early Svecofennian age (ca 1.9 Ga). Most of the metavolcanic rocks were originally deposited as SiO_2-rich pyroclastics, but remnants of lava flows and subvolcanic intrusions are also present. The metasedimentary units include mica schists, quartzites and marbles. Most ores (Fe oxide and base-metal sulphide deposits) are hosted by metavolcanic rocks that commonly have been hydrothermally altered at an early, volcanic stage. Some mineralization occurs in metacarbonate layers. The supracrustal units are intruded by two generations of plutonic rocks. The older (1.90–1.85 Ga) intrusions are dominantly felsic (tonalite to monzogranite in composition) and normally foliated or gneissic. The younger intrusive rocks (1.80–1.78 Ga) are essentially undeformed, relatively homogeneous granite *sensu stricto*. Some pegmatites in the area appear to belong to the later generation. The supracrustal and older intrusive rocks were metamorphosed in lower to middle amphibolite facies and underwent ductile deformation in connection with the Svecofennian orogeny at *ca.* 1.85 Ga. Later tectonic stress caused fracturing and faulting in the area.

In the Norberg District, NW Västmanland, lanthanide mineralizations have been reported from a number of now-abandoned Fe mines: the two most important being Malmkärra and Östanmossa (Geijer, 1927, 1961). The deposits consist of disseminated magnetite-amphibole skarn replacements in marble. Major minerals sequestering lanthanides are allanite-(Ce), dissakisite-(Ce), dollaseite-(Ce), fluorbritholite-(Ce) and bastnäsite-(Ce) (Holtstam & Andersson, 2002). Geijer (1927) reported cerite, but our studies indicate that the mineral in part may have been confused with fluorbritholite, which was not identified previously at these localities. The Östanmossa deposit is the type locality for dollaseite-(Ce) (Peacor & Dunn, 1988), first named "magnesium orthite" by Geijer (1927). Fluorine-rich minerals, such as norbergite, chondrodite, fluorian phlogopite, and fluorite, are commonly associated with the lanthanide minerals (Geijer, 1927; Holtstam & Andersson, 2002).

At the Bastnäs deposit, Skinnskatteberg District, W Västmanland, quartz-banded hematite ore occurs in close proximity to magnetite-skarn ore, the latter replacing a carbonate layer (Geijer, 1923). Lanthanide minerals were encountered in two small mines that transect a restricted skarn zone composed mainly of cerite-(Ce), tremolitic amphibole, ferriallanite-(Ce), bastnäsite-(Ce), törnebohmite-(Ce), talc and various Cu-Bi-Mo sulphide minerals. At Rödbergsgruvan, Örebro County, the lanthanide mineralization has not been described from an *in situ* occurrence. Dump material consists of tremolite skarns with cerite-(Ce), ferriallanite-(Ce), bastnäsite-(Ce), molybdenite, and chalcopyrite.

Sample descriptions

All samples have been examined in polished thin sections under a polarizing microscope, and an energy-dispersive X-ray microanalyser was used as an aid in mineral identification. The type specimen (Malmkärra, #01+0081) consists mainly of dark red to grayish fluorbritholite-(Ce), nearly black västmanlandite-(Ce), a bluish-green serpentine mineral, tremolite, dolomite, and magnetite. Individual grains of västmanlandite-(Ce) range from 0.2 to 3 mm in their greatest dimension. They are usually anhedral, but crystals adjacent to patches of dolomite tend to be euhedral. Fluorbritholite-(Ce), in the form of larger irregular aggregates and subrounded grains, is embayed by tremolite-serpentine and occasionally dolomite. The fine-grained serpentine

Table 1. Electron microprobe analyses (wt.% oxide) of västmanlandite-(Ce) and related minerals.

Sample no.	01+0081				381132	970319	880072	52:414	A037
				mean	*n* = 2	*n* = 4	*n* =2	*n* = 2	*n* = 2
La_2O_3	13.97	13.85	13.13	13.65	18.74	14.29	17.16	17.62	15.68
Ce_2O_3	23.92	23.58	24.22	23.90	22.20	23.29	21.86	21.57	22.83
Pr_2O_3	1.95	2.15	2.10	2.07	1.43	1.89	1.55	1.52	1.52
Nd_2O_3	6.16	6.28	6.40	6.28	3.82	5.39	4.01	4.08	4.31
Sm_2O_3	0.35	0.48	0.45	0.42	0.16	0.52	0.26	0.28	0.23
Gd_2O_3	0.14	0.18	0.14	0.15	0.01	0.27	0.17	0.07	0.05
Dy_2O_3	0.01	0.01	0.01	0.01	0.05	0.12	0.05	0.02	0.07
Ho_2O_3	0.03	0.00	0.03	0.02	0.01	0.04	0.02	0.06	0.00
Er_2O_3	0.00	0.00	0.00	0.00	0.02	0.09	0.04	0.00	0.01
Yb_2O_3	0.07	0.00	0.02	0.03	0.02	0.04	0.00	0.01	0.00
Y_2O_3	0.18	0.21	0.14	0.18	0.12	0.78	0.26	0.06	0.04
CaO	4.73	4.49	4.72	4.65	4.69	4.20	4.39	4.53	4.66
FeO*	2.88	3.96	3.84	3.56	2.75	3.75	8.93	10.01	11.37
MgO	5.83	5.51	5.19	5.51	6.37	5.84	3.11	2.02	1.46
Al_2O_3	8.68	8.28	8.77	8.58	8.82	8.38	7.91	8.27	7.77
SiO_2	26.90	26.31	26.63	26.61	26.48	26.87	25.80	25.96	25.80
P_2O_5	0.05	0.05	0.04	0.05	0.02	0.16	0.02	0.07	0.05
TiO_2	0.03	0.04	0.05	0.04	0.03	0.03	0.02	0.05	0.04
F	1.17	1.06	0.97	1.06	1.59	1.29	0.71	0.21	0.21
Sum	97.02	96.43	96.82	96.75	97.33	97.23	96.24	96.39	96.07
O=F	-0.49	-0.45	-0.41	-0.45	-0.67	-0.54	-0.30	-0.09	-0.09
Total	96.53	95.98	96.41	96.31	96.66	96.68	95.94	96.31	95.98
	Formula contents based on 13 cations								
La	0.950	0.954	0.898	0.934	1.269	0.972	1.199	1.231	1.105
Ce	1.615	1.612	1.644	1.624	1.492	1.573	1.516	1.496	1.596
Pr	0.131	0.146	0.142	0.140	0.096	0.127	0.107	0.105	0.105
Nd	0.406	0.419	0.424	0.416	0.251	0.355	0.271	0.276	0.294
Sm	0.022	0.031	0.028	0.027	0.010	0.033	0.017	0.018	0.015
Gd	0.009	0.011	0.008	0.009	0.001	0.017	0.010	0.004	0.003
Dy	0.000	0.001	0.001	0.001	0.003	0.007	0.003	0.001	0.004
Ho	0.002	0.000	0.001	0.001	0.000	0.002	0.001	0.003	0.000
Er	0.000	0.000	0.000	0.000	0.001	0.005	0.002	0.000	0.001
Yb	0.004	0.000	0.001	0.002	0.001	0.002	0.000	0.001	0.000
Y	0.018	0.021	0.014	0.017	0.012	0.076	0.026	0.006	0.004
Ca	0.935	0.898	0.938	0.924	0.923	0.831	0.891	0.920	0.953
Sum *A***	4.092	4.093	4.100	4.095	4.058	4.002	4.044	4.060	4.079
Fe	0.445	0.618	0.595	0.552	0.423	0.578	1.414	1.586	1.815
Mg	1.602	1.535	1.433	1.524	1.742	1.607	0.878	0.571	0.416
Sum Fe+Mg	2.047	2.153	2.028	2.076	2.165	2.186	2.293	2.158	2.231
Al	1.887	1.823	1.916	1.875	1.909	1.823	1.767	1.846	1.749
Si	4.964	4.917	4.942	4.942	4.862	4.961	4.890	4.918	4.929
P	0.007	0.008	0.006	0.007	0.003	0.025	0.003	0.012	0.007
Ti	0.004	0.005	0.007	0.005	0.004	0.004	0.003	0.007	0.005
Sum cations	13.000	13.000	13.000	13.000	13.000	13.000	13.000	13.000	13.000
F	0.680	0.624	0.568	0.624	0.923	0.754	0.428	0.124	0.126

Note: *n* = number of point analyses. *Fe measured as FeO. **A = Ca + the lanthanides.

mineral has apparently formed from pervasive breakdown of amphibole. Magnetite, as subequant grains up to 2 mm across, is commonly associated with västmanlandite-(Ce). Some grains of västmanlandite-(Ce) have a poikiloblastic texture, with microscopic inclusions of magnetite, fluorbritholite-(Ce), partly altered amphibole, and dollaseite-(Ce) (Fig. 1). The enclosed magnetite is sometimes oxidized to hematite along grain boundaries. Textural relations in thin sections indicate that västmanlandite-(Ce) has formed at the expense of fluorbritholite-(Ce) and amphibole.

A more complete account of the parageneses of the lanthanide minerals at the Bastnäs-type deposits will be given elsewhere. Samples other than the holotype material that contain minerals of the västmanlandite series are included in this work mainly to discuss important chemical substitutions. Their mineral assemblages are summarized in the following list:

#970319, Malmkärra: fluorbritholite-(Ce), dollaseite-(Ce), gadolinite-(Ce), tremolite, chalcopyrite, pyrite, arsenopyrite.

#381132, Södra Hackspikgruvan (a small, presently inaccessible mine close to Östanmossa, Norberg): fluorbritho-

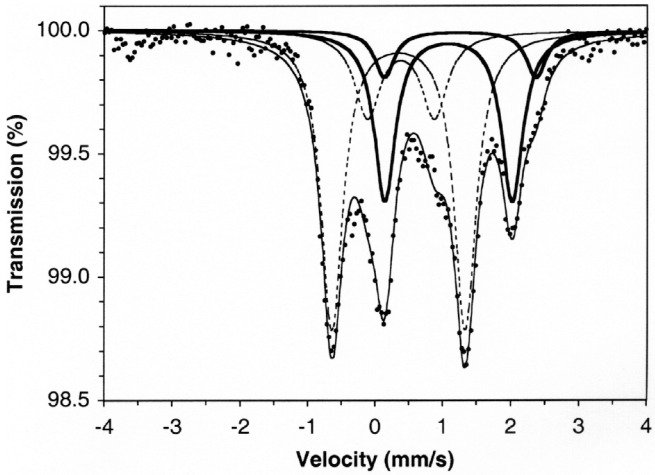

Fig. 3. Fitted Mössbauer spectrum of västmanlandite-(Ce). Dashed lines represent the quadrupole Fe^{3+} subspectra, solid black the Fe^{2+} subspectra. The thin black line represents the sum of all four subspectra.

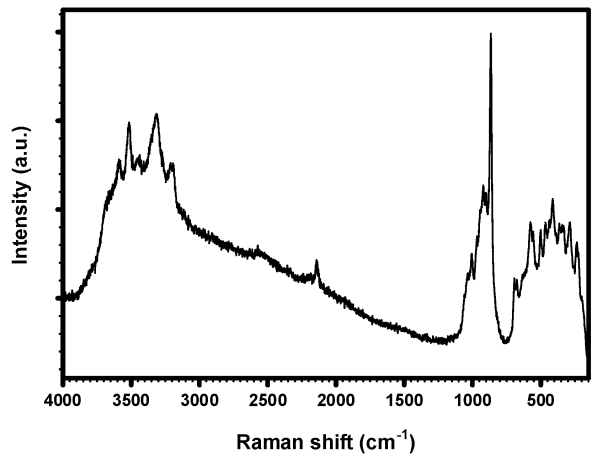

Fig. 4. Single-crystal Raman spectrum of västmanlandite-(Ce).

lite-(Ce), bastnäsite-(Ce), dollaseite-(Ce), fluorite, tremolite, phlogopite, magnetite, molybdenite.

#880072, Rödbergsgruvan: cerite-(Ce), ferriallanite-(Ce), bastnäsite-(Ce), tremolite, zircon.

#52:414, Bastnäs: cerite-(Ce), bastnäsite-(Ce), bismuthinite, chalcopyrite, quartz.

#A037, Bastnäs: cerite-(Ce), ferriallanite-(Ce), törnebohmite-(Ce), bastnäsite-(Ce), talc, amphibole, fluocerite-(La), cerianite.

Physical and optical properties

In the type specimen, västmanlandite-(Ce) is black to dark brown, translucent with a vitreous luster, and its streak is yellowish gray. Cleavage is good along {001}, and fracture is uneven to conchoidal. The Mohs hardness is approximately 6. The crystals seem to be unaffected by cold conc. HCl and HNO_3. The calculated density of the mineral (based on the empirical formula) is 4.51(2) g·cm^{-3}. Optically, it is biaxial negative with $\alpha = 1.781(4)$, $\beta = 1.792$(calc.), $\gamma = 1.810(4)$ at $\lambda = 589$ nm and $2V_{\alpha} = 75(5)°$. The dispersion is strong with $r > v$. The mineral is strongly pleochroic, with the scheme *X* pale yellow, *Y* reddish brown, *Z* dark brown, and absorption $Z \sim Y > X$ (orientation unknown). The compatibility index calculated from the Gladstone-Dale relationship is 0.003, which falls in the "superior" category (Mandarino, 1981). In general, västmanlandite-(Ce) is very similar in its macroscopic and microscopic character to certain varieties of non-metamict allanite; therefore chemical and diffraction analysis will be necessary in most cases for a confirmation.

Table 2. Mössbauer data for västmanlandite-(Ce).

Sub-spectrum	*CS** (mm/s)	*QS*** (mm/s)	Γ (mm/s)	*Abs. area* (%)
Fe^{3+}(A)	0.35	1.97	0.38	51(4)
Fe^{3+}(B)	0.39	0.99	0.38	16(2)
Fe^{2+}(A)	1.09	1.88	0.38	26(3)
Fe^{2+}(B)	1.26	2.22	0.38	7(2)

*centroid shift. **quadrupole split.

Chemical composition and spectroscopic data

The chemical composition of the new mineral was determined using wavelength dispersive quantitative analyses on a Cameca SX50 electron microprobe at GeoForschungsZentrum, Potsdam, Germany, run with an accelerating voltage of 20 kV, a beam current of 40 nA and a 3-μm beam diameter. Standards used were pure synthetic REE phosphates (REE*L*β), YPO_4 (Y*L*α) Fe_2O_3 (Fe*K*α), $MnTiO_3$ (Ti*K*α), wollastonite (Ca, Si*K*α), $PrPO_4$ (P*K*α), Al_2O_3 (Al*K*α), MgO (Mg*K*α), and LiF (F*K*α). Each peak was measured for 30 or 50 seconds (10 and 25 seconds for the background, respectively). Data reduction was carried out using a Cameca version of the PAP (Pouchou & Pichoir, 1991) routine. Na, Cl, Mn, Sr, Ba, Lu, Th, and U contents were below the limits of detection (≤ 0.05 wt.%) in all points. Results from three point analyses of the type specimen and average analytical values for five other samples are given in Table 1. The empirical formulae in the table have been calculated on the basis of 13 cations; the formula of the type specimen is $(Ce_{1.62}La_{0.93}Nd_{0.42}Pr_{0.14}Sm_{0.03}Y_{0.02}Gd_{0.01})_{\Sigma 3.17}Ca_{0.92}Mg_{1.52}Fe^{2+}_{0.18}Fe^{3+}_{0.37}Al_{1.88}Si_{4.94}P_{0.01}O_{19}(OH)_2(F_{0.62}O_{0.38})$. The H_2O concentration is estimated at 1.6 wt.% assuming the presence of 2 OH^-. The samples analyzed are relatively constant in Si and Al, with ranges 4.86–4.96 and 1.75–1.92 atoms pfu (per formula unit), respectively. Ca and lanthanide contents are fairly homogeneous as well, with Ce > La > Nd > Pr for the complete population. This is in contrast with the associated fluorbritholite-(Ce) in the two specimens from Malmkärra, that consistently have Ce > Nd > La > Pr. Large variations, even within individual samples, are found only for Mg, Fe and F. A clear antipathetic relation between F + Mg and Fe is shown diagrammatically in Fig. 2.

A transmission ^{57}Fe Mössbauer spectroscopy measurement was carried out on a 50-mg sample, purified by handpicking and magnetic extraction from the holotype specimen. An X-ray powder diffractometer pattern recorded

Table 3. X-ray powder diffraction data for västmanlandite-(Ce).

I_{meas}	I_{calc}	d_{meas}(Å)	d_{calc}(Å)	h	k	l
16	80	15.81	15.79	0	0	$\overline{1}$
7	23	7.99	8.03	1	0	$\overline{1}$
3	5	7.86	7.89	0	0	$\overline{2}$
2	8	7.50	7.51	1	0	1
2	5	6.14	6.15	1	0	2
5	9	4.792	4.800	1	1	0
8	11	4.688	4.696	1	0	$\overline{3}$
10	32	4.651	4.648	1	1	$\overline{1}$
	12		4.621	0	1	$\overline{2}$
2	4	4.387	4.381	1	0	3
	2		4.377	2	0	$\overline{1}$
5	9	4.176	4.181	1	1	$\overline{2}$
3	4	4.012	4.016	2	0	$\overline{2}$
3	7	3.939	3.947	0	0	$\overline{4}$
2	4	3.858	3.867	0	1	$\overline{3}$
3	<1	3.541	3.540	2	0	$\overline{3}$
20	46	3.503	3.509	2	1	0
7	23	3.473	3.474	1	1	3
4	8	3.375	3.381	2	1	1
3	11	3.281	3.283	2	1	$\overline{2}$
	4		3.274	2	0	3
2	5	3.112	3.115	1	1	$\overline{4}$
4	20	3.072	3.077	2	0	$\overline{4}$
100	100	2.9831	2.9869	1	1	4
4	8	2.8751	2.8760	3	0	1
10	43	2.8507	2.8497	0	2	0
6	1	2.8426	2.8439	2	0	4
2	5	2.8032	2.8044	0	2	$\overline{1}$
8	32	2.7622	2.7621	0	1	$\overline{5}$
3	4	2.7078	2.7085	3	0	2
13	20	2.6852	2.6857	1	2	$\overline{1}$
11	28	2.6784	2.6775	2	0	$\overline{5}$
19	57	2.6250	2.6267	3	1	$\overline{1}$
4	5	2.5479	2.5478	1	2	2
2	4	2.5066	2.5059	0	2	$\overline{3}$
4	11	2.4485	2.4463	3	1	2
	5		2.4369	1	2	$\overline{3}$
8	8	2.2856	2.2869	3	0	4
6	3	2.2790	2.2775	2	1	5
5	14	2.2717	2.2696	2	2	2
4	4	2.2541	2.5555	0	0	$\overline{7}$
15	17	2.1874	2.1882	4	0	$\overline{2}$
7	2	2.1812	2.1806	4	0	1
8	24	2.1489	2.1494	2	2	3
3	10	2.1158	2.1156	0	2	$\overline{5}$
5	2	2.1017	2.0996	4	0	2
7	5	2.0970	2.0972	0	1	$\overline{7}$
	7		2.0958	3	1	$\overline{5}$
10	19	2.0907	2.0907	2	2	$\overline{4}$
	2		2.0838	1	2	$\overline{5}$
6	5	2.0819	2.0794	2	0	$\overline{7}$
3	1	2.0759	2.0757	4	1	$\overline{1}$
2	3	2.0554	2.0556	3	2	0
6	4	1.9938	1.9944	4	0	3
2	2	1.9692	1.9702	4	1	2
5	19	1.9502	1.9513	2	2	$\overline{5}$
	5		1.9503	2	0	7
4	11	1.9314	1.9332	3	1	$\overline{6}$
	2		1.8952	1	0	8
4	4	1.8945	1.8940	4	1	4
2	7	1.8738	1.8727	2	2	5
7	15	1.8542	1.8533	1	1	$\overline{8}$
6	4	1.8494	1.8488	1	3	$\overline{1}$

Note: The pattern is indexed based on calculated intensities from structure refinement.

before the powder was transformed into a tablet indicated that the absorber material consisted of > 95 % of västmanlandite and was free from magnetite. Two mirror-image spectra with a velocity span of ± 4.3 mm/s calibrated against α-iron were collected at magic-angle geometry (54.7°) over 1024 channels (Fig. 3). Spectrum analysis was carried out under the assumption of a "thin" absorber and Lorentzian line shapes (Jernberg & Sundqvist, 1983). The lines were constrained to equal widths (Γ). The best fit (χ^2 = 2.2) was obtained with four doublets attributed to two sets each of Fe^{2+} and Fe^{3+}, from their centroid shift values (Table 2). From the area proportions, the amount of ferric iron is estimated at 67(5) % of total Fe present; details are discussed further below.

Single-crystal laser-Raman spectra were recorded from small grains with random orientation (Fig. 4). A Renishaw MicroRaman Imaging system (M1000) was used with a laser wavelength of 633 nm and excitation through a Leica DMLM optical microscope. Spectra were recorded between 100 and 4000 cm^{-1} with a spectral resolution of ± 2 cm^{-1} and a minimum lateral resolution of ~2 μm on the sample. All grains proved to be stable under the laser beam.

X-ray diffraction studies and structure determination

X-ray powder diffraction

X-ray powder diffraction data were recorded with step scans in the 2θ-range 3 to 80° (0.02° and 10 seconds per step) on an automated Philips PW1710 diffractometer using graphite-monochromatized Cu$K\alpha$ radiation (PW1830 generator operated at 40 kV and 40 mA). Peak positions were determined with the X'Pert Graphics & Identify program and corrected against an external Si standard (NBS 640b). Indexed d values for reflections with 2θ ≤ 50° and relative peak heights above background for the holotype specimen of västmanlandite-(Ce) are given in Table 3. The pattern is indexed on the basis of intensities calculated from the crystal-structure determination (*vide infra*). The monoclinic unit-cell parameters, refined from fifty-five reflections using a least-squares program (Novak & Colville, 1989), are a = 8.932(2), b = 5.699(2), c = 15.838(6) Å, β = 94.54(4)° and V = 804(1) Å^3.

Table 4. Crystal data, data collection information and refinement details for västmanlandite-(Ce).

Crystal data	
Space group	$P2_1/m$ (no. 11)
a, b, c(Å)	8.939(1), 5.706(1), 15.855(2)
β(°)	94.58(1)
V(Å^3), Z	806.1(2), 2
F(000), ρ_{calc}(g · cm^{-3})	1005, 4.46
μ (mm^{-1})	9.960
Absorption correction	multi-scan*
Crystal dimensions (mm)	0.06 x 0.07 x 0.07
Data collection	
Diffractometer	Nonius KappaCCD system
λ (Mo-$K\alpha$) (Å), T(K)	0.71073, 293
Crystal-detector dist. (mm)	40
Rotation axes; width (°)	φ, ω; 1.0
Total no. of frames	1071
Collect. time per frame (s)	120
Collection mode, $2\theta_{max}$(°)	sphere, 65.08
h, k, l ranges	$\overline{13}\rightarrow13$, $\overline{8}\rightarrow8$, $\overline{24}\rightarrow23$
Total reflections measured	5837
Unique reflections	3171 (R_{int}1.30%)
Refinement	
Refinement on	F^2
$R1(F)$, w$R2(F^2)$**, w$R2(F^2)_{all}$	1.73 %, 3.89 %, 4.16 %
'Observed' refls.	2864 [$F_o > 4\sigma(F_o)$]
Extinct. coefficient	0.0016(1)
No. of refined parameters	210
GooF	1.081
$(\Delta/\sigma)_{max}$	0.001
$\Delta\rho_{min}$, $\Delta\rho_{max}$(e/Å^3)	-0.90, 0.89

Note: Unit-cell parameters were refined from 3177 reflections. Scattering factors for neutral atoms were employed in the refinement. *Otwinowski & Minor (1997); minimum and maximum transmission factors: 0.542 and 0.586. **w = $1/[\sigma^2(F_o^2) + (0.01P)^2 + 1.34P]$; P = ([max of (0 or$F_o^2$)] + $2F_c^2$)/3.

Single-crystal X-ray diffraction and structure solution

Several optically homogeneous crystal fragments from the type material were mounted on a Nonius KappaCCD single-crystal four-circle X-ray diffractometer equipped with a 300-μm diameter capillary-optics collimator to provide increased resolution. All fragments showed sharp diffraction maxima and an identical primitive monoclinic cell. On the recorded CCD frames of all fragments, an extremely weak, continuous streaking parallel to c^* at $a^*/2$ was observed (often clearly visible only on severely overexposed CCD frames); the intensity of these continous streaks was *ca.* 2–5 times background-intensity, with no recognizable diffraction maxima along the streaking. Essentially identical, albeit slightly stronger streaking was also observed for grains of the Fe-dominant analogue of västmanlandite-(Ce). These phenomena, explained by the very close structural relation to gatelite-(Ce), are discussed below.

Intensity data from a suitable, nearly equi-dimensional crystal fragment of type västmanlandite-(Ce) were collected at room temperature using Mo-$K\alpha$ radiation (see Table 4 for details). The measured data were processed with the Nonius program suite DENZO-SMN and corrected for Lorentz-polarization, background, and absorption effects. Systematic extinctions and normalized structure-factor statistics indicated the centrosymmetric space group $P2_1/m$, with refined unit-cell parameters a = 8.939(1), b = 5.706(1), c = 15.855(2) Å, β = 94.58(1)°, V = 806.1(2) Å^3, and Z = 2. The crystal structure was determined by direct methods (SHELXS-97, Sheldrick, 1997a) and has been refined on F^2 (SHELXL-97, Sheldrick, 1997b) in space group $P2_1/m$. Refinement proceeded smoothly and conversion to anisotropic displacement factors for the cation sites resulted in a preliminary $R1(F)$ of ca. 11 %. At this stage, all occupancies of the cation sites were carefully refined on the basis of crystal-chemical considerations (bond-lengths, bond-valence sums) and the relation to gatelite-(Ce) and the epidote group; the "split" nature of two adjacent sites (Ce3 and O15) was taken into account, and all anion sites were refined anisotropically. Hydrogen atoms could not be located. The final structure model shows good agreement with the empirical chemical formula. Details of the model, and the fact that it represents only an average structure, are discussed in more detail below. The final residuals were $R1(F)$ = 1.73 % and w$R2(F^2)$ = 3.89 % for 2864 'observed' reflections with $F_o > 4\sigma(F_o)$. Maximum and minimum peaks in the final difference-Fourier maps were 0.89 and –0.90 e/Å^3, respectively. Positional parameters are given in Tables 5a–c (Table 5c is deposited and available directly from the authors or the EJM editorial office in Paris), and selected bond lengths and angles in Table 6. An empirical bond-valence analysis is presented in Table 7. A list of the observed and calculated structure factors can be obtained from the authors.

Description of crystal structure and crystal-chemical relations

A brief, preliminary description of the crystal structure of västmanlandite-(Ce) was given by Kolitsch *et al.* (2002). The structure is nearly isotypic to that of the recently described mineral gatelite-(Ce), ideally $Ce_3CaAl_2AlMg[Si_2O_7][SiO_4]_3O(OH)_2$ (Bonazzi *et al.*, 2003), although västmanlandite-(Ce) has a different space group and unit cell (the intricate structural relationship between both minerals is explained in more detail in the discussion section). The new root name is justified mainly on the basis of the difference in cation composition, Al_2AlMg *vs.* Al_2Mg_2. Following Bonazzi *et al.* (2003), gatelite-(Ce) is based on a regularly alternating stakking of an epidote-type module (E) [Dollase, 1969, 1971; Carbonin & Molin, 1980; Peacor & Dunn, 1988; Catti *et al.*, 1989; Grew *et al.*, 1991; Rouse & Peacor, 1993; Bonazzi & Menchetti, 1995] and a törnebohmite-(Ce) module (T) [$(Ce,La)_2Al(SiO_4)_2(OH)$, (Shen & Moore, 1982)]. Specifically, gatelite-(Ce) is an ET polysome within a polysomatic series having dissakisite-(Ce) [$Ca(Ce,La)MgAl_2(SiO_4)_3(OH)$, Grew *et al.*, 1991; Rouse & Peacor, 1993] and törnebohmite-(Ce) as end members (Bonazzi *et al.*, 2003). Correspondingly, västmanlandite-(Ce) can be considered as a regular dollaseite-(Ce)–törnebohmite-(Ce) polysome [dollaseite-(Ce) = $CaCeMg_2AlSi_3O_{11}F(OH)$, Peacor & Dunn, 1988].

Table 5a. Atom coordinates and equivalent displacement parameters (Å^2) for västmanlandite-(Ce).

Atom	*x*	*y*	*z*	U_{eq}	Refined occupancy
Ce1	0.85943(2)	3/4	0.25017(1)	0.01084(5)	Ce^{3+}*
Ce2	0.58997(2)	1/4	0.16558(1)	0.00953(5)	Ce^{3+}*
Ce3**	0.77129(3)	0.7200(1)	0.00960(1)	0.0110(2)	0.5(Ce^{3+}*)
Ca	0.18223(6)	3/4	0.40937(3)	0.0110(2)	Ca:Ce = 0.922(1):0.078(1)
Mg1 (*M*1)	1/2	1/2	1/2	0.0064(2)	Mg:Fe = 0.812(3):0.188(3)
Mg2 (*M*3)	0.68719(9)	1/4	0.37631(5)	0.0090(2)	Mg:Fe = 0.746(3):0.254(3)
Al (*M*2)	0.22646(7)	-0.4992(1)	0.20392(4)	0.0070(2)	Al:Fe = 0.964(2):0.036(2)
Si1	0.82068(9)	3/4	0.47627(5)	0.0064(1)	
Si2	0.03461(9)	1/4	0.33421(5)	0.0060(1)	
Si3	0.50998(9)	3/4	0.31233(5)	0.0056(1)	
Si4	0.93385(9)	1/4	0.10290(5)	0.0078(2)	
Si5	0.42363(9)	-1/4	0.07729(5)	0.0063(1)	
O1	0.7230(2)	0.5074(3)	0.4789(1)	0.0100(3)	
O2	0.6130(2)	0.5243(3)	0.29111(9)	0.0090(3)	
O3	0.1104(2)	0.4859(3)	0.2984(1)	0.0104(3)	
F***	0.4792(2)	1/4	0.41700(1)	0.0047(3)	(F,O)
O5	0.5416(2)	1/4	0.5902(1)	0.0087(4)	
O6	0.3460(2)	3/4	0.2565(1)	0.0093(4)	
O7	0.9209(3)	3/4	0.3973(1)	0.0108(4)	
O8	0.8597(3)	1/4	0.3066(2)	0.0177(5)	
O9	0.0659(3)	1/4	0.4369(1)	0.0156(5)	
OH1	0.3500(2)	1/4	0.2461(1)	0.0085(4)	OH
O11	0.34201(2)	-0.4900(3)	0.1083(1)	0.0120(3)	
OH2	0.1033(2)	3/4	0.1620(1)	0.0085(4)	OH
O13	0.8915(2)	3/4	-0.1470(1)	0.0090(4)	
O14	0.8386(2)	0.4744(3)	0.1316(1)	0.0161(3)	
O15**	0.9521(3)	0.3273(6)	0.0049(2)	0.0132(6)	0.5 O
O16	0.4166(4)	-1/4	-0.0230(2)	0.0351(8)	
O17	0.5949(3)	-1/4	0.1173(2)	0.0224(6)	

Note: Mg1, Mg2, and Al correspond to the *M*1, *M*3, and *M*2 sites, respectively, in epidote-group minerals. *Ce^{3+} includes other REE^{3+} ions. **Ce3 and O15 form pairs of two mirror-related atoms, Ce3/Ce3' and O15/O15' (see text and Table 6). ***A tentative refinement of the occupancy of the F site gave a F:O ratio of about 0.5:0.5 (see text). A very minor amount of OH may also be present on the F site.

The structural relationship between västmanlandite-(Ce) and epidote-group minerals is most easily recognized when viewing the structures of västmanlandite-(Ce) and dollaseite-(Ce) along their respective **b**-axes (Fig. 5). Västmanlandite-(Ce) is a (Ce,La)-Ca-Al-(Mg,Fe)-F-silicate containing lanthanide (mainly Ce^{3+}) and Ca sites, chains of $AlO_4(OH)_2$ octahedra parallel to the **b**-axis, and chains of $(Mg,Fe)O_4(F,O)_2$ octahedra with $(Mg,Fe)O_5(F,O)$ octahedra attached on alternate sides along their length. These composite chains also parallel the **b**-axis. SiO_4 tetrahedra and Si_2O_7 groups connect the cation polyhedra to form a three-dimensionally bonded structure. The H atoms of the two OH groups (OH1 and OH2) could not be located with sufficient certainty. The chemical composition suggested by the refinement is $Ce^*_3[Ca_{0.92}Ce^*_{0.08}]_{\Sigma 1.00}{}^{[M1]}(Mg_{0.81}Fe_{0.19})_{\Sigma 1.00}{}^{[M3]}(Mg_{0.75}Fe_{0.25})_{\Sigma 1.00}{}^{[M2]}(Al_{1.92}Fe_{0.08})_{\Sigma 2.00}Si_5O_{19.00}(OH)_2(F,O)_{1.00}$ (* including all other REE), where the accepted site designations of epidote-group minerals (*M*1, *M*2, and *M*3) are given as superscripts. This formula is in good agreement with the formula calculated from the electron microprobe and Mössbauer data (see above and Table 1).

Västmanlandite contains three lanthanide sites, of which the Ce3 site forms a pair of two mirror-related (x,y,z and x,-y,z) Ce3 atoms with a very short interatomic distance [Ce3–Ce3' = 0.343(2) Å], each of which is half-occupied in the average structure (for explanation see sections further below). These three lanthanide sites are occupied by REE^{3+} cations. Ca is not present at them according to refinements of the site occupancies. Average Ce-O bond lengths range between 2.635 and 2.711 Å (Table 6). Furthermore, there is one Ca site for which refined site occupancies indicate 92.2(1)% Ca and 7.8(1)% lanthanide cations, and which has an average (Ca, REE)-O bond length of 2.467 Å. All samples analyzed show a deficit in Ca in comparison to the ideal structural formula, and there is a fair negative correlation (linear $R = 0.54$) for Ca *vs.* (REE-3). This feature is probably related to the common allanite-type coupled substitution $Ca + M^{3+} = REE + M^{2+}$. As for the smaller cations, there is one Al site with refined occupancy ratio Al:Fe = 0.964(2):0.036(2), and two (Mg,Fe) sites with refined occupancy ratios of Mg:Fe = 0.812(3):0.188(3) for Mg1 and Mg:Fe = 0.746(3):0.254(3) for Mg2. Average bond lengths for these three sites are 1.910 (Al), 2.007 (Mg1), and 2.109 (Mg2) Å (Table 6). Mg1, Mg2, and Al correspond to the *M*1, *M*3, and *M*2 sites, respectively, in the epidote-group minerals.

The Si and O atoms in västmanlandite-(Ce) have been labeled as in the epidote-type structure, as far as possible. There are five Si sites, 16 O sites and one F site. The SiO_4 tetrahedra have average Si–O bond lengths ranging from

Table 5b. Anisotropic displacement parameters (in Å^2) for västmanlandite-(Ce).

Atom	U_{11}	U_{22}	U_{33}	U_{23}	U_{13}	U_{12}
Ce1	0.00922(8)	0.01636(9)	0.00705(8)	0	0.00133(6)	0
Ce2	0.00869(8)	0.01298(8)	0.00702(8)	0	0.00116(6)	0
Ce3	0.01480(10)	0.0121(5)	0.00610(9)	-0.0004(1)	0.00049(7)	0.0009(1)
Ca	0.0103(3)	0.0115(3)	0.0107(3)	0	-0.0027(2)	0
Mg1	0.0066(4)	0.0049(4)	0.0077(4)	0.0007(3)	0.0015(3)	0.0005(3)
Mg2	0.0108(4)	0.0085(4)	0.0081(4)	0	0.0020(3)	0
Al	0.0065(3)	0.0062(3)	0.0085(3)	-0.0001(2)	0.0019(2)	-0.0004(2)
Si1	0.0068(3)	0.0061(3)	0.0063(3)	0	0.0007(3)	0
Si2	0.0055(3)	0.0064(3)	0.0063(3)	0	0.0006(3)	0
Si3	0.0042(3)	0.0066(3)	0.0059(3)	0	0.0008(3)	0
Si4	0.0052(3)	0.0111(4)	0.0069(3)	0	0.0001(3)	0
Si5	0.0065(3)	0.0064(3)	0.0064(4)	0	0.0021(3)	0
O1	0.0094(7)	0.0082(7)	0.0124(7)	0.0008(5)	0.0009(5)	-0.0016(5)
O2	0.0083(6)	0.0094(7)	0.0093(7)	-0.0009(5)	0.0009(5)	0.0023(5)
O3	0.0125(7)	0.0073(7)	0.0119(7)	0.0002(5)	0.0044(6)	-0.0008(6)
F	0.0054(9)	0.0039(8)	0.0048 (9)	0	0.0012(7)	0
O5	0.009(1)	0.0086(9)	0.0085(9)	0	0.0021(8)	0
O6	0.0067(9)	0.0089(9)	0.012(1)	0	-0.0021(8)	0
O7	0.011(1)	0.012(1)	0.010(1)	0	0.0036(8)	0
O8	0.007(1)	0.033(1)	0.013(1)	0	0.0006(8)	0
O9	0.014(1)	0.023(1)	0.009(1)	0	-0.0032(8)	0
OH1	0.0065(9)	0.010(1)	0.009(1)	0	0.0009(7)	0
O11	0.0118(7)	0.0079(7)	0.0172(8)	0.0001(6)	0.0061(6)	-0.0012(6)
OH2	0.0075(9)	0.0088(9)	0.009(1)	0	0.0009(7)	0
O13	0.0048(9)	0.011(1)	0.011(1)	0	-0.0004(7)	0
O14	0.0086(7)	0.0091(7)	0.030(1)	-0.0008(7)	-0.0035(6)	0.0011(6)
O15	0.013(1)	0.017(1)	0.009(1)	0.002(1)	-0.001(1)	-0.0004(11)
O16	0.044(2)	0.054(2)	0.007(1)	0	0.003(1)	0
O17	0.007(1)	0.040(1)	0.021(1)	0	0.0015(9)	0

1.619 (Si2) to 1.642 (Si3) Å (Table 6). The O15 site, which provides a connection between the mirror-related Ce3/Ce3' atom pair and Si4, also forms a pair of two mirror-related (x,y,z and x,-y,z) O15 atoms with a very short interatomic distance [O15-O15' = 0.882(6) Å], and accordingly each of those sites is half-occupied in the average structure.

As in the Mg-members of the epidote group, the Mg2 (*M*3) site contains more Fe than the Mg1 (*M*1) site. The $Mg2O_5F$ octahedron is also more distorted than the $Mg1O_4F_2$ octahedron. The hyperfine Mössbauer parameters (Table 2) suggest distribution over two sites for both Fe^{3+} and Fe^{2+}. The Fe^{3+}(B) spectrum (dashed in Fig. 3) is assigned to the Al site from its low quadrupole splitting, which is in accordance with a less distorted site in terms of *M*–O distances. This corresponds to 16 % of total Fe, or 0.09 Fe atoms pfu, in agreement with the Fe occupancy obtained from the structure refinement, 0.08 atoms pfu. Both Fe^{2+} and Fe^{3+} are expected to be present on the two Mg sites. From the sizes of coordination polyhedra it seems probable that Fe^{3+} prefers the Mg1 (*M*1) site, although in epidote-group minerals Fe^{3+} generally seems to prefer the site equivalent to Mg2 (*M*3). Nonetheless, in the new epidote-group member ferriallanite-(Ce), $CaCeFe^{3+}AlFe^{2+}(SiO_4)(Si_2O_7)O(OH)$ (Kartashov *et al*., 2002; Holtstam *et al*., 2003b), Fe^{3+} also seems to prefer the *M*1 site.

The two Fe^{2+} doublets are likely to correspond to Fe^{2+} ions distributed over Mg1 and Mg2 (solid lines in Fig. 3). The 1.26 mm/s centroid shift value for Fe^{2+}(B) is somewhat high for Fe^{2+} in [6]-coordination. A possible explanation is that the smaller fraction of this ionic species is located at Mg1, where the two F ligands, being more electronegative than O, are expected to contribute to a higher centroid shift value (Shenoy, 1984). An enrichment of Fe^{2+} at Mg2 can also be expected from a comparison of the calculated bond valences (Table 7).

The F contents measured by EPMA, 1.06 wt. % on average, are attributed to a specific site denoted F, which corresponds to the "O4" anion site in dollaseite-(Ce), $CaCeMg_2AlSi_3O_{11}F(OH)$, where F > O (Peacor & Dunn, 1988). A good correlation between the measured Mg, Fe and F contents, particularly if results from the analyses of the larger sample population are considered, clearly suggests the substitution Mg + F = Fe^{3+} + O in västmanlandite-(Ce) (*cf.* Fig. 2), and, consequently, the presence of both F and O on the "F" site is implied. A tentative refinement of the F:O ratio on this site gave 0.461(4):0.539(4), but the actual standard uncertainties are certainly much larger, and the refined F:O ratio must be considered unreliable.

The predominance of fluorine on the F site may also explain the short Mg1-F bond length of 1.940(1) Å (Table 6). Because the actual F content and the accurate Fe^{2+}:Fe^{3+} ratio of the crystal fragment used for intensity measurements are not known, the calculation of the bond-valence sums (BVS) for Mg1 and Mg2 is only possible on a qualitative basis (see

Table 6. Selected bond distances (Å) and bond angles (°) for the coordination polyhedra in västmanlandite-(Ce).

Ce1–O7	2.354(2)	Ce2–O16	2.256(3)
–O14 x2	2.447(2)	–O2 x2	2.527(2)
–O2 x2	2.6759(2)	–OH1	2.582(2)
–OH2	2.682(2)	–O14 x2	2.657(2)
–O3 x2	2.760(2)	–O11 x2	2.760(2)
–O8 x2	2.9902(9)	–O17 x2	2.9552(8)
–O17	3.039(3)	<Ce2–O>	2.664
<Ce1–O>	2.711		
Ce3*–Ce3'*	0.343(2)	Ca–O7	2.329(2)
Ce3*–O17	2.421(3)	–O3 x2	2.366(2)
–O14	2.424(2)	–O1 x2	2.403(2)
–O11	2.4370(2)	–O5	2.468(2)
–O15*	2.516(3)	–O6	2.930(2)
–O15*	2.575(3)	<Ca–O>	2.467
–O14	2.637(2)		
–O11	2.637(2)		
–O15*	2.767(3)		
–O13	2.789(2)		
–O15	3.054(3)		
<Ce3–O>	2.635		
Mg1–F x2	1.940(1)	Mg2–O8	1.968(2)
–O5 x2	2.033(2)	–F	2.016(2)
–O1 x2	2.048(2)	–O2 x2	2.138(2)
<Mg1–O>	2.007	–O1 x2	2.196(2)
		<Mg2–O>	2.109
Al–OH2	1.886(2)	Si1–O7	1.596(2)
–O3	1.890(2)	–O1 x2	1.639(2)
–OH1	1.896(2)	–O9	1.643(2)
–O11	1.902(2)	<Si1–O>	1.629
–O6	1.928(2)		
–O13	1.955(2)		
<Al–O>	1.910		
Si2–O8	1.589(2)	Si3–O2 x2	1.634(2)
–O9	1.629(2)	–O5	1.647(2)
–O3 x2	1.630(2)	–O6	1.651(2)
<Si2–O>	1.619	<Si3–O>	1.642
Si4–O14 x2	1.623(2)	Si5–O16	1.587(3)
–O15* x2	1.636(3)	–O17	1.610(3)
–O13	1.659(2)	–O11 x2	1.645(2)
<Si4–O>	1.635	<Si5–O>	1.622
O15*–O15'*	0.882(6)		
angle of disilicate group:		Si2-O9-Si1	151.9(2)

Note: Mg1, Mg2, and Al correspond to the *M*1, *M*3, and *M*2 sites, respectively, in epidote-group minerals. *Ce3 and O15 form pairs of mirror-related atoms, Ce3/Ce3' and O15/O15'.

Table 7). If the F sites were completely occupied by O atoms, the BVS of Mg1 would be much too high (2.592 v.u.), and the presence of Fe (Fe^{2+} and/or Fe^{3+}) on this site would increase this value further. If F is assumed to be completely occupied by fluorine, a more reasonable BVS of 2.083 v.u. is obtained. The BVS for Mg1 and Mg2 in Table 7, 2.61 and 2.08 v.u., were calculated assuming Fe = Fe^{3+} on both (Mg,Fe) sites and a F:O ratio of 1:1 on the F site. The presence of Fe^{2+} and a higher F:O ratio would reduce these values.

Interpretation of Raman spectroscopic data

A typical single-crystal laser-Raman spectrum (Fig. 4) shows a complex cluster of mostly broadened bands at ~ 3671 (shoulder), ~3586, 3517, ~3446, ~3317 (asymmetric) and ~3201 cm^{-1} in the OH stretching region. This suggests at least six different local environments for the hydroxyl groups detected and agrees with the structure refinement (OH groups on the OH1 and OH2 sites, and possibly also in very minor amounts on the F site). Because the OH1 and OH2 sites can have different neighbours (Al and/or Fe on neighbouring Al sites), slightly different band positions will result. The wave-numbers of the observed bands indicate the presence of OH...O hydrogen bonds with distances ranging from roughly 2.7 to 3.3 Å, according to the correlation curve established by Libowitzky (1999). These distances show reasonably good agreement with those determined experimentally (OH...O > 2.8 Å). At lower wave-numbers, two small reproducible peaks at ~2545 and ~2142 cm^{-1} are presently unexplained. The presence of fluorescence bands caused by REE^{3+} ions may explain these peaks. No attempts to use other wavelengths or to measure in the anti-Stokes region were made. The 1100–150 cm^{-1} region is very complex and shows no similarity to spectra of epidote-group minerals. In particular, the region between 700 and 150 cm^{-1} shows a complex association of bands reflecting the complex character of a three-dimensional structure with a large unit cell and low symmetry. The bands are observed at ~690, ~675, ~633, 574, 555, 501, 464, ~436, 412, 387, 361, 341, 329, 287, 234, 224 and ~200 cm^{-1}. The 750–1100 cm^{-1} region represents the stretching vibrational regime of the SiO_4 and Si_2O_7 groups. A very strong band is observed at 865 cm^{-1}, accompanied by medium to weak bands at 900, 920, ~944, 968, 1004, 1034 and ~1058 cm^{-1}. An attempt to give a complete assignment of all bands is beyond the scope of the present work.

Discussion

Relation to gatelite-(Ce)

Västmanlandite-(Ce), ideally $(Ce,La)_3CaAl_2Mg_2[Si_2O_7][SiO_4]_3F(OH)_2$, is nearly isotypic to gatelite-(Ce), ideally $Ce_3CaAl_2AlMg[Si_2O_7][SiO_4]_3O(OH)_2$ (Bonazzi *et al.*, 2003). Although the two species have different space groups and unit-cell parameters (västmanlandite-(Ce): $P2_1/m$, a = 8.939(1), b = 5.706(1), c = 15.855(2) Å, β = 94.58(1)°, V = 806.1(2) $Å^3$; gatelite-(Ce): $P2_1/a$, with a = 17.770(4), b = 5.651(1), c = 17.458(4) Å, β = 116.18(2)°, V = 1573.3(6) $Å^3$), they share the same overall topology and can be considered as nearly isotypic (see below for an explanation). The unit cell of västmanlandite-(Ce) can be transformed into a gatelite-type cell by the matrix (-2 0 0, 0 -1 0, 1 0 1); this gives the cell a' = 17.878(1), b' = 5.706(1), c' = 17.569(2) Å, β' = 115.90(1)°, V' = 1612.2(3) $Å^3$ (space group $P2_1/a$). The transformation causes the Al, O1 and O2 sites to split into pairs of sites, but leads to the merging of the two pairs of mirror-related atoms with very short interatomic distances (Ce3/Ce3' and O15/O15') into two single, unsplit atoms (Ce3 and O15). Con-

Table 7. Empirical bond-valence analysis of västmanlandite-(Ce).

	Ce1	Ce2	Ce3*	Ca	Mg1	Mg2	Al	Si1	Si2	Si3	Si4	Si5	Sum
O1				0.308 x2	0.397 x2	0.270 x2		0.961 x2					1.94***
O2	0.242 x2	0.362 x2				0.315 x2				0.973 x2			1.89***
O3	0.193 x2			0.340 x2			0.524		0.984 x2				2.04
F**					0.496 x2 x2	0.407							1.40***
O5				0.258	0.413 x2 x2					0.940			2.02***
O6				0.074			0.473 x2			0.930			1.98
O7	0.578			0.376				1.079					2.03
O8	0.104 x2 x2					0.499			1.099				1.81***
O9								0.950	0.987				1.94
OH1		0.312					0.516 x2						1.34
O11		0.193 x2	0.462, 0.269				0.507					0.944 x2	1.98
OH2	0.238						0.529 x2						1.30
O13			0.178 x2				0.440 x2				0.910		1.97
O14	0.449 x2	0.254 x2	0.478, 0.269								1.004 x2		2.08
O15*			0.373, 0.318, 0.189, 0.087								0.968		1.94
O16		0.753										1.105	1.86
O17	0.092	0.114 x2 x2	0.482 x2									1.039	1.84
Sum	2.88	2.91	2.76	2.00	2.61***	2.08***	2.99	3.95	4.05	3.82	3.89	4.03	

Note: Bond-valence parameters used are from Brese & O'Keeffe (1991) and, for Fe^{3+}-F bonds, recently improved bond-valence parameters (program VALENCE by Brown, 1996; updated parameters list from 2002). Values have been calculated taking into account the refined occupancies for the Mg1 and Mg2 sites (Mg:Fe ratios 0.818(3):0.182(3) and 0.750(3):0.250(3), respectively), the split character of the Ce3 and O15 sites, and using the bond-valence parameters of Ce^{3+} for the three Ce sites (see Table 3 and text); the very minor Fe^{3+} content on the Al site has been neglected (it would increase the BVS to 3.03 v.u.). *Ce3 and O15 form pairs of two mirror-related atoms, Ce3/Ce3' and O15/O15' (see Tables 5a, 6). **F represents a mixture of F and O. ***Calculated assuming Fe = Fe^{3+} on both (Mg,Fe) sites and a F:O ratio of 1:1 on the F site.

versely, the unit cell of gatelite-(Ce) can be transformed into a västmanlandite-type cell by the matrix (-0.5 0 0, 0 -1 0, 0.5 0 1); the resulting cell has a' = 8.885(4), b' = 5.651(1), c' = 15.712(4) Å, β' = 94.32(2)°, V' = 786.6(3) Å^3.

The average structure of västmanlandite-(Ce)

Two features indicate that the obtained structure model of västmanlandite-(Ce) represents only an average structure. Firstly, the extremely weak continuous streaking parallel to c^* at $a^*/2$ (Fig. 6), which was observed for both västmanlandite-(Ce) and its Fe analogue, is evidence for a local (short-range) doubling of the **a**–axis, *i.e.*, a tendency to adopt the unit cell of gatelite-(Ce). However, the extreme weakness of the continuous streaking in västmanlandite-(Ce) is in strong contrast with the weak, although apparently sharp superstructure reflections in gatelite-(Ce) which must be caused by long-range atomic ordering of those atoms offset from the mirror planes in $P2_1/m$ (Bonazzi *et al.*, 2003).

Secondly, the existence of the two pairs of mirror-related atoms in västmanlandite-(Ce), Ce3/Ce3' and O15/O15', can only be explained by an average structure. In the gatelite model (see deposited Table 5c and explanatory footnote), there are no such pairs. Both "split" Ce3 and O15 sites belong to the törnebohmite-(Ce) module (T) in västmanlandite-(Ce) (see Fig. 5). Thus, locally two geometrically slightly different arrangements of Ce3 and O15 are present in the T-modules. These arrangements are apparently not ordered and consequently lead only to continuous streaks of intensity parallel to c^*, but not to superstructure reflections. It may be assumed that the ordered atomic arrangement in gatelite-(Ce) mainly involves an ordering of the Ce3 site (*A3* site of Bonazzi *et al.*, 2003) in the törnebohmite-(Ce) module. This would also correlate with the fact that in both törnebohmite-(Ce) and gatelite-(Ce) slight offsets of atoms in the T module from the mirror planes in $P2_1/m$ lead to weak superstructure reflections and a deviation from (ideal) space-group symmetry $P2_1/m$ to space group $P2_1/c$ for törnebohmite-(Ce) and $P2_1/a$ for gatelite-(Ce) (Bonazzi *et al.*, 2003).

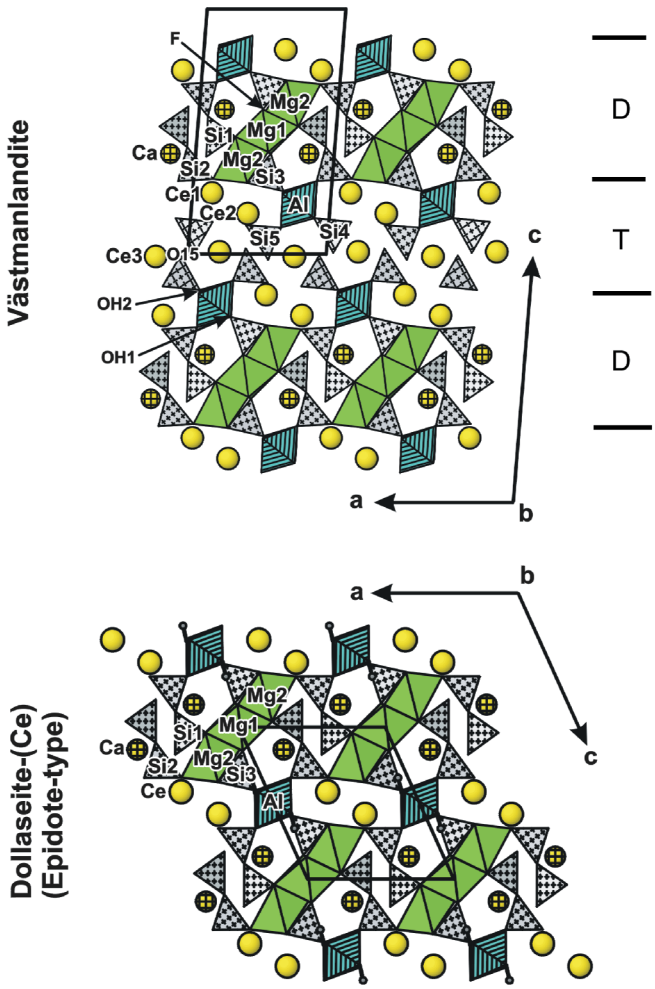

Fig. 5. Comparison of the structures of västmanlandite-(Ce) and dollaseite-(Ce) in a view along [010] and [0$\bar{1}$0], respectively. Unit cells of each structure are shown. The orientations of the dollaseite-(Ce) module (D) and the törnebohmite-(Ce) module (T) in västmanlandite-(Ce) are schematically indicated. Ce atoms are yellow, Ca atoms are yellow and cross-hatched, $(Mg,Fe)(O,F)_6$ octahedra are green, $AlO_4(OH)_2$ octahedra are turquoise and striped, SiO_4 tetrahedra are gray and marked with crosses, and H atoms are represented by small gray spheres. Note that Mg1, Mg2 and Al correspond to the *M*1, *M*3, and *M*2 sites in epidote-group minerals (see also text and Tables 5a and 5c). In västmanlandite-(Ce), both the Ce3 and O15 sites form pairs of two mirror-related atoms, Ce3/Ce3' and O15/O15', with very short interatomic distances (this results from the necessary description of the atomic arrangement as an average structure, see text for details). F represents a mixture of F and O; OH1 and OH2 are two OH groups on the $AlO_4(OH)_2$ octahedral chains.

A qualitative explanation for the extreme weakness of the continuous streaking in västmanlandite-(Ce) might be given by the offset of only two atoms (Ce3 and O15) from the (010) mirror plane, unlike in gatelite-(Ce) where many more atoms show this offset, ultimately resulting in weak, although sharp superstructure reflections (Bonazzi *et al.*, 2003). The dominant reason for the streak-inducing disorder in västmanlandite-(Ce) may be the fairly high temperature at which the mineral crystallized (see section on Genetic aspects).

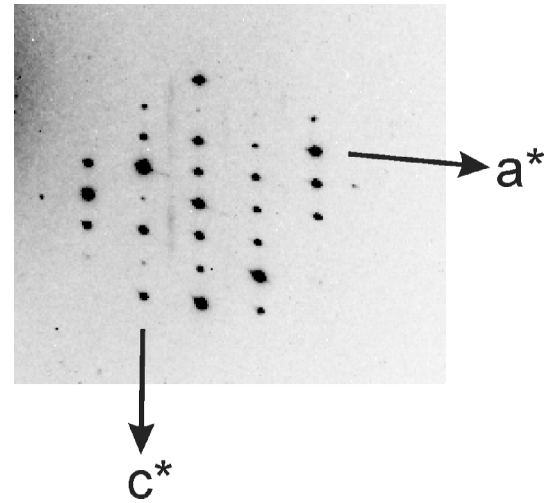

Fig. 6. Single-crystal X-ray diffraction pattern of västmanlandite-(Ce) in a view nearly parallel to *b** (severely overexposed digital CCD frame). Note the extremely weak continuous streaking indicating a local (short-range) doubling of the **a**-axis (see text for discussion).

It should be noted that the extremely weak streaking in västmanlandite-(Ce) would probably not be visible on diffraction patterns obtained by standard X-ray film methods (*i.e.*, with 'normal' exposure times). Furthermore, the lack of indexable superstructure reflections will cause automated single-crystal diffractometers to always yield the västmanlandite-type unit cell, but not a gatelite-type unit cell.

Chemical composition of västmanlandite-(Ce)

The present sample population shows no solid solution of västmanlandite-(Ce) towards gatelite-(Ce), due to the lack of Al on the octahedral Mg1 and Mg2 positions of the crystal fragment subjected to structure refinement, and from the fact that all samples have Al < 2 atoms pfu. Instead, the chemical and structural data of västmanlandite-(Ce) indicate the presence of a second end-member possessing the structure type of västmanlandite-(Ce) with the ideal composition $Ce_3CaAl_2Fe^{3+}Mg[Si_2O_7][SiO_4]_3O(OH)_2$, which would be the Fe^{3+}-O analogue of västmanlandite-(Ce). Our preliminary study indicates that Fe-rich and F-poor samples along the solid solution series (*cf.* Fig. 2) have the same $P2_1/m$ structure (including the extremely weak continuous streaks) with unit-cell parameters similar to those obtained for västmanlandite-(Ce), but with Fe > Mg on both Mg1 and Mg2 sites (the accurate Fe^{3+}:Fe^{2+} ratio in these samples is not known yet). The substitution Mg + F = M^{3+} + O, which relates the composition of dollaseite $[CeCaMg_2Al(Si_2O_7)(SiO_4)F(OH)]$ with that of allanite $[(Ce,La,Y)CaFe^{2+}(Al,Fe^{3+})_2(Si_2O_7)(SiO_4)O(OH)]$ (Peacor & Dunn, 1988), and operates in specimens chemically corresponding to the series dollaseite-(Ce)–dissakisite-(Ce) from the Bastnäs-type deposits (Holtstam & Andersson, unpublished), apparently applies to västmanlandite-(Ce) as well. F^-–O^{2-} substitution is rare in the mineral kingdom, but occurs to a limited extent in other silicates, *e.g.*, garnets (Valley *et al.*,

1983) and meliphanite (Grice & Hawthorne, 2002). It should be noted that the famous "Fe^{2+}-F avoidance rule", reported in the literature for micas and amphiboles (*e.g.*, Rosenberg & Foit, 1977), is not applicable here because of the coupled substitution involving Fe^{3+} and O^{2-}.

In the chemical-structural classification system of Strunz & Nickel (2001), västmanlandite-(Ce) and gatelite-(Ce) are silicates that would belong to the subdivision 9.BG (sorosilicates with mixed SiO_4 and Si_2O_7 groups; cations in octahedral and greater coordination). Theoretically, the crystal structure of västmanlandite-(Ce) would allow other cationic substitutions than indicated here, and a whole group of minerals with this structure type might be recognized in the future.

Genetic aspects

What factors control the formation of this mineral? The lanthanide mineralization at the Bastnäs-type deposits is generally considered to have the form of metasomatic skarns, resulting from the interaction between hydrothermal lanthanide-enriched fluids and carbonate (dolomitic) rocks (Geijer, 1961). The absence of quartz in equilibrium with the lanthanide minerals in the present mineral assemblages is noteworthy, and the crystallization of västmanlandite-(Ce) and its Fe-O analogue is probably favoured in silica-undersaturated systems. The fluorine activity appears to be particularly critical. The incorporation of F is not only governed by structural factors, but also controlled by the Fe^{2+}/Fe^{3+} ratio and then indirectly by the prevailing oxygen fugacity during the formation of västmanlandite-(Ce). The presence of oxidized rims on magnetite grains enclosed by västmanlandite-(Ce) suggests oxygen fugacity levels above the hematite-magnetite buffer in the present case.

In its general crystal-chemical features, the new mineral is most similar to dollaseite-(Ce) (in fact, its E module), and possibly only relatively slight variations in the availability of the major components decide which of the two minerals crystallizes. For example, västmanlandite-(Ce) is more effective in hosting lanthanides than dollaseite-(Ce) and should then be favoured by higher lanthanide activities in the system. The pressure and temperature conditions are essentially unknown, although one could expect fairly high temperatures in the original, skarn-forming fluids (> 400°C). The petrographic data indicate that västmanlandite-(Ce) formed in secondary reactions involving fluorbritholite-(Ce) and tremolite as the principal reactants, although Al was to be supplied from an outside source.

Acknowledgements: Special thanks are due to Tobbe and Otto Wikström, who secured the "cerite" specimen from Malmkärra. Donald R. Peacor and Giovanni Ferraris provided helpful comments on the manuscript. Earlier versions of the manuscript benefitted from reviews by Paul Evins, Paola Bonazzi and Roberta Oberti. The Swedish Research Council (VR) financially supported this work. U.K. gratefully acknowledges support of the Deutsche Forschungsgemeinschaft (DFG) via a Research Fellowship and of the Austrian Science Foundation (FWF; grant P15220-GEO). Oona Appelt at GeoForschungsZentrum (GFZ), Potsdam, was most helpful during the microprobe analyses, performed while U.B.A. upheld a post-doctoral fellowship at GFZ granted by STINT (Stiftelsen för internationalisering av högre utbildning och forskning).

References

Allen, R.L., Lundström, I., Ripa, M., Simeonov, A.H. (1996): Facies analysis of a 1.9 Ga, continental margin, back-arc, felsic caldera province with diverse Zn-Pb-Ag-(Cu-Au) sulfide and Fe oxide deposits, Bergslagen region, Sweden. *Econ. Geol.*, **91**, 979-1008.

Ambros, M. (1983): Beskrivning till berggrundskartan Lindesberg NO. *Sver. Geol. Undersök.*, **Af 141**, 1-75. (in Swedish)

– (1988): Beskrivning till berggrundskartorna Avesta NV och SV. *Sver. Geol. Undersök.,* **Af 152-153**, 1-84. (in Swedish)

Bonazzi, P. & Menchetti, S. (1995): Monoclinic members of the epidote group: effects of the $Al \leftrightarrow Fe^{3+} \leftrightarrow Fe^{2+}$ substitution and of the entry of REE^{3+}. *Mineral. Petrol.*, **53**, 133-153.

Bonazzi, P., Bindi, L., Parodi, G. (2003): Gatelite-(Ce), a new REE-bearing mineral from Trimouns, French Pyrenees: Crystal structure and polysomatic relationship with epidote and törnebohmite-(Ce). *Am. Mineral.*, **88**, 223-228.

Brese, N.E. & O'Keeffe, M. (1991): Bond-valence parameters for solids. *Acta Crystallogr.*, **B47**, 192-197.

Brown, I.D. (1996): VALENCE: a program for calculating bond valences. *J. Appl. Crystallogr.*, **29**, 479-480.

Carbonin, S. & Molin, G. (1980): Crystal-chemical considerations on eight metamorphic epidotes. *N. Jahrb. Mineral., Abh.*, **139**, 205-215.

Catti, M., Ferraris, G., Ivaldi, G. (1989): On the crystal chemistry of strontian piemontite with some remarks on the nomenclature of the epidote group. *N. Jahrb. Mineral., Monatsh.*, **1989**, 357-366.

Dollase, W.A. (1969): Crystal structure and cation ordering of piemontite. *Am. Mineral.*, **54**, 710-717.

– (1971):Refinement of the crystal structures of epidote, allanite, and hancockite. *Am. Mineral.*, **56**, 477-464.

Geijer, P. (1921): The cerium minerals of Bastnäs at Riddarhyttan. *Sver. Geol. Undersök.*, **C304**, 1-24.

– (1923): Geologisk beskrivning. *in* "Riddarhytte malmfält i Skinnskattebergs socken i Västmanlands län". Kungl. Kommerskollegium & Sveriges Geologiska Undersökning. Victor Pettersson, Stockholm, 1-138. (in Swedish)

– (1927): Some mineral associations from the Norberg district. *Sver. Geol. Undersök.*, **C343**, 1-32.

– (1961): The geological significance of the cerium mineral occurrences of the Bastnäs type in Central Sweden. *Ark. Min. Geol.*, **3**, 99-105.

Grew, E.S., Essene, E.J., Peacor, D.R., Su, S.C., Asami, M. (1991): Dissakisite-(Ce), a new member of the epidote group and the magnesium analogue of allanite-(Ce), from Antarctica. *Am. Mineral.* **76**, 1990-1997.

Grice, J.D. & Hawthorne, F.C. (2002): New data on meliphanite, $Ca_4(Na,Ca)_4Be_4AlSi_7O_{24}(F,O)_4$. *Can. Mineral.*, **40**, 971-980.

Holtstam, D. (2002): Cobaltkieserite, $CoSO_4 \cdot H_2O$, a new mineral species from Bastnäs, Skinnskatteberg, Sweden. *GFF,* **124**, 117-119.

Holtstam, D. & Andersson, U.B. (2002): Rare earth mineralogy of Bastnäs-type Fe-REE(-Cu-Mo): deposits in Bergslagen, Sweden. Abstracts, International Mineralogical Association 18th General Meeting, Edinburgh, p. 282.

Holtstam, D. & Broman, C. (2002): Lanthanide mineralizations of Bastnäs type: overview and new data. *GFF*, **124**, 230-231.

Holtstam, D., Norrestam, R., Andersson, U.B. (2003a): Percleveite-(Ce), a new lanthanide disilicate mineral from Bastnäs, Skinnskatteberg, Sweden. *Eur. J. Mineral.*, **15**, 725-731.

Holtstam, D., Andersson, U.B., Mansfeld, J. (2003b): Ferriallanite-(Ce) from the Bastnäs deposit, Västmanland, Sweden. *Can. Mineral.*, **41**, 1233-1240.

Ibers, J.A. & Hamilton, W.C. (1974): International Tables for X-ray Crystallography, vol. IV. Kynoch Press, Birmingham, 356 p.

Jernberg, P. & Sundqvist, T. (1983): A versatile Mössbauer analysis program. University of Uppsala, Institute of Physics Report, UU-IP-1090.

Kartashov, P.M., Ferraris, G., Ivaldi, G., Sokolova, E., McCammon, C.A. (2002): Ferriallanite-(Ce), $CaCeFe^{3+}AlFe^{2+}(SiO_4)(Si_2O_7)O(OH)$, a new member of the epidote group: description, X-ray and Mössbauer study. *Can. Mineral.*, **40**, 1641-1648.

Kolitsch, U., Holtstam, D., Andersson, U.B. (2002): The crystal structure of a new REE-Ca-Mg,Fe-Al-F-silicate from Sweden and its close relation to the epidote structure type. *Berichte der Deutschen Mineralogischen Gesellschaft, Beih. z. Eur. J. Mineral.*, **14**, No. 1, 88.

Libowitzky, E. (1999): Correlation of O-H stretching frequencies and O-H···O hydrogen bond lengths in minerals. *Monatsh. Chem.*, **130**, 1047-1059.

Mandarino, J.A. (1981): The Gladstone-Dale relationship. IV. The compatibility concept and its application. *Can. Mineral.*, **19**, 441-450.

Novak, G.A. & Colville, A.A. (1989): A practical interactive least-squares cell-parameter program using an electronic spreadsheet and a personal computer. *Am. Mineral.*, **74**, 488-490.

Otwinowski, Z. & Minor, W. (1997): Processing of X-ray diffraction data collected in oscillation mode. *Methods Enzymol.*, **276**, 307-326.

Peacor, D.R. & Dunn, P.J. (1988): Dollaseite-(Ce) (magnesium orthite redefined): Structure refinement and implications for $F + M^{2+}$ substitutions in epidote-group minerals. *Am. Mineral.*, **73**, 838-842.

Persson, L. (1997): Beskrivning till berggrundskartorna Avesta SO och NO. *Sver. Geol. Undersök.*, **Af 189, 197**, 1-69. (in Swedish)

Pouchou, J.-L. & Pichoir, F. (1991): Quantitative analysis of homogeneous or stratified microvolumes applying the model "PAP". *in* "Electron Probe Quantitation", K.F.J. Heinrich & D.E. Newbury, eds. Plenum Press, New York, 31-75.

Ripa, M., Kübler, L., Persson, L., Göransson, M. (2002): Beskrivning till berggrundskartan Västerås 11G NO. *Sver. Geol. Undersök.*, **Af 217**, 1-70. (in Swedish)

Rosenberg, P.E. & Foit, F.F. (1977): Fe^{2+}–F avoidance in silicates. *Geochim. Cosmochim. Acta*, **41**, 345-346.

Rouse, R.C. & Peacor, D.R. (1993): The crystal structure of dissakisite-(Ce), the magnesium analogue of allanite-(Ce). *Can. Mineral.*, **31**, 153-157.

Sheldrick, G.M. (1997a): SHELXS-97, a program for the solution of crystal structures. University of Göttingen, Germany.

– (1997b): SHELXL-97, a program for crystal structure refinement. University of Göttingen, Germany.

Shen, J. & Moore, P. B. (1982): Törnebohmite, $RE_2Al(OH)[SiO_4]_2$: crystal structure and genealogy of RE(III)Si(IV) ↔ Ca(II)P(V) isomorphism. *Am. Mineral.*, **67**, 1021-1028.

Shenoy, G.K. (1984): Mössbauer-effect isomer shifts. *in* "Mössbauer spectroscopy applied to inorganic chemistry", G.J. Long, ed. Plenum Press, New York , vol. 1, 57-76.

Strunz, H. & Nickel, E.H. (2001): "Strunz Mineralogical Tables. Chemical-Structural Classification system". 9th edition, Schweizerbart'sche Verlagsbuchhandlung, Stuttgart, 870 p.

Valley, J.W., Essene, E.J., Peacor, D.R. (1983): Fluorine-bearing garnets in Adirondack calc-silicates. *Am. Mineral.*, **68**, 444-448.

Received 23 September 2003
Modified version received 4 August 2004
Accepted 30 August 2004